CrystEngComm

Accepted Manuscript

ROYAL SOCIETY OF CHEMISTRY

www.rsc.org/crystengcomm

Cite this: DOI: 10.1039/c0xx00000x

www.rsc.org/xxxxxx

ARTICLE TYPE

The phosphorescent cocrystals of 1,4-diiodotetrafluorobenzene and bent 3-ring-N-hetrocyclic hydrocarbons by C-I···N and C-I···π halogen bonds

Hui Wang, Ruo Xin Hu, Xue Pang, Hai Yue Gao, Wei Jun Jin*

Received (in XXX, XXX) Xth XXXXXXXXX 20XX, Accepted Xth XXXXXXXXX 20XX
DOI: 10.1039/b000000x

The cocrystals **1-3** were successfully assembled by 1,4-diiodotetrafluorobenzene (1,4-DITFB) and bent 3-ring-N-hetrocyclic hydrocarbons (3-R-NHHs) based on halogen bond (XB) and other weak interactions. The halogen bond as a good strategy of introducing metal-free heavy atom perturber in stoichiometry is further confirmed, which makes the spin-orbital coupling more efficient and the phosphorescence more observable. Herein, the selected 3-R-NHHs in cocrystals **1-3** are differently emitting green, orange yellow and orange phosphorescence with well defined vibrational bands at 544 nm (max) for **1**, 592 nm (max) for **2** and 605 nm (max) for **3**, whereas the pure 3-R-NHHs are not phosphorescent in the solid state. The reason can be mainly ascribed to that the different N-positions in three 3-R-NHHs affect C-I···π halogen bond properties which influence further the energy level of excited triplet state and meanwhile make the transition from T_1 to higher vibrational level of S_0 state become more probable with respective to the free monomer. It is estimated that in the cocrystals the energy level of excited ππ* triplet state is lowered as evidenced by the presence of a bathochromic effect in maximum emission bands of 50 ~ 100 nm. The other interactions and local molecular environment can affect the phosphorescence behaviours, too. The different phosphorescence behaviours of three cocrystals should be suitable to design some appropriate π-type acceptors for developing phosphorescence materials *via* halogen bonds.

Introduction

The design and preparation of optical cocrystal materials have been one of the hottest topics of current research due to potential and real needs.[1-3] In general, aromatic molecules and a handful of unsaturated aliphatic molecules with π-conjugation electronic structure are strongly light-emitting organic compounds in solution. However, due to the quench caused by forming excimers or exciplexes, these pure organic luminophores usually become weak or non-emissive in solid or film.[4,5] Moreover, it is difficult to effectively emit phosphorescence with long lifetime for them because the singlet-triplet transition is spin-forbidden. Therefore, it is necessary to adopt a strategy to promote the singlet-triplet conversion, and it is also an extremely challenging task to construct new solid phosphorescence materials.[3,6,7] Currently, the halogen bond (XB)[8] as a kind of important intermolecular interaction has been applied in many fields, such as molecular recognition,[9,10] preparation of magnetic materials[11,12] and photoresponsive materials,[13] *etc*. Interestingly, typical halogen bond donors, for example, I or Br atom in organic molecules, can be considered as an efficient way of introducing metal-free efficient heavy atom perturber to organic luminophores in certain stoichiometry. Based on the consideration, Kim group[14,15] prepared a group of strong phosphorescence materials with tuneable colors.

In our group, Gao et al[16] first prepared a novel organic phosphorescent cocrystal by 1,4-DITFB and carbazole using C-I···π XB. Later, a cocrystal is also successfully assembled on the synergistic effect of C-I···N XB and π-hole···F bond.[17] The co-crystallization can not only promote phosphorescence, but also modulate the phosphorescent spectra and the corresponding decay kinetics in a certain degree. So, it is necessary and significant to explore the luminescence behaviours of those cocrystal materials containing NHHs further. Herein three bent 3-R-NHH systems with excited singlet/triplet state of ππ* characters are selected as XB acceptors and they are not phosphorescent in the solid state. The XRD reveals that the main driving forces of cocrystals **1-3** assembled by 3-R-NHHs and 1,4-DITFB are C-I···N/π XB. These cocrystals are differently emitting strong green, orange yellow and orange phosphorescence, respectively, due to the different C-I···π XB. It is expected that this study should play a key role in designing some appropriate π-type acceptors to assemble strong

College of Chemistry, Beijing Normal University, Beijing 100875, P. R. China. E-mail: wjjin@bnu.edu.cn, Tel/Fax: (+86)10-58802146.
† Electronic Supplementary Information (ESI) available: Additional Figures, Tables and data. CCDC: 975980-975982. See DOI:10.1039/b000000x/

phosphorescence materials and enrich the practical applications of halogen bond in functionalized materials, particularly in the solid luminescent materials field.

Experimental

Reagents

1,4-Diiodotetrafluorobenzene (1,4-DITFB, 98%), Phenanthridine (PHN, 98%), Benzo[f]quinoline (BfQ, 98%) and Benzo[h]quinoline (BhQ, 99%) were purchased from TCI Co. (Tokyo, Japan). Their structures of halogen bonding donor/acceptors are showed in **Scheme 1**. All the other reagents are of analytical purity grade and used without further purification.

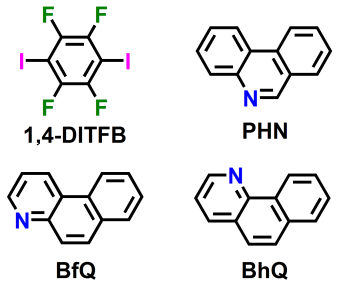

Scheme 1 Structures of halogen bonding donor (D) and acceptors (A). The stoichiometries of D/A in cocrystals are 1:2 (1,4-DITFB:PHN), 1:1 (1,4-DITFB:BfQ) and 3:2 (1,4-DITFB:BhQ), respectively.

Preparation of cocrystals

Cocrystal ***1.*** 1,4-DITFB and PHN in 1:1 and 1:2 ratios were dissolved in acetone solvent in a glass vial. Slow evaporation of the solvent at room temperature for about three weeks all yielded isostructural colorless crystals. The product was isolated prior to total evaporation of the solvent to guarantee the crystal purity. Melting point: 149.4 °C. FT-IR: ν_{max} 1460, 1239, 1210, 942, 892, 754, 571 cm^{-1}. Raman (solid): ν_{max} 1037, 714, 554, 502, 152 cm^{-1}. Elemental analysis: Calcd/found (%) for $C_{16}H_9F_2IN$: C, 50.55/50.73; H, 2.39/2.42; N, 3.69/3.73.

Cocrystal ***2.*** 1,4-DITFB and BfQ in 1:1 and 1:2 ratios were dissolved in a 4:1 acetone/chloroform mixture solvent in a glass vial. Slow evaporation of the solvent at room temperature for about three weeks all yielded isostructural colorless crystals. The product was isolated prior to total evaporation of the solvent to guarantee the crystal purity. Melting point: 117.5 °C. FT-IR: ν_{max} 1460, 1386, 1300, 1212, 942, 871, 750, 565 cm^{-1}. Raman (solid): ν_{max} 1061, 1039, 712, 556, 502, 155 cm^{-1}. Elemental analysis: Calcd/found (%) for $C_{19}H_9F_4I_2N$: C, 39.27/39.35; H, 1.56/1.52; N, 2.41/2.87.

Cocrystal ***3.*** 1,4-DITFB and BhQ in 1:1 and 1:2 ratios were dissolved in acetone solvent in a glass vial. Slow evaporation of the solvent at room temperature for about three weeks all yielded isostructural colorless crystals. The product was isolated prior to total evaporation of the solvent to guarantee the crystal purity. Melting point: 65.8 °C. FT-IR: ν_{max} 1463, 1402, 1216, 945, 836, 750, 568 cm^{-1}. Raman (solid): ν_{max} 1209, 1039, 1018, 712, 499, 411, 243, 156 cm^{-1}. Elemental analysis: Calcd/found (%) for $C_{22}H_9F_6I_3N$: C, 33.78/34.76; H, 1.16/1.17; N, 1.79/2.29.

Crystallography

The single crystal data of cocrystal **1-3** were collected at 295 K on a Bruker SMART APEX diffractometer with Mo-Kα radiation (λ 0.71073 Å) and graphite monochromator operating in the multi-scan. The structures were resolved by direct method and refined by full matrix least-squares on F^2 using SHELXTL program with anisotropic thermal parameters for all non-hydrogen atoms.[18,19] Hydrogen atoms were included at estimated positions and refined using calculation positions. Single crystal data were listed in **Table 1**.

XRPD

X-ray powder diffraction (XRPD) patterns were obtained at 293 K on an XPert Pro MPD diffractometer with a Cu-Kα Enhance Ultra source (λ 1.5418 Å). The ground cocrystal powders were dried for 24 h under vacuum at room temperature. The simulated patterns were generated from the single-crystal structure by the OriginPro 8.

Spectroscopic measurements

All phosphorescence spectra were recorded on a Cary Eclipse spectrophotometer (Varian) equipped with a flashed xenon lamp and with a 1 mm ×10 mm quartz cuvette at a 30/60° angle for the powder samples or ground cocrystals. The excitation wavelengths were set at 352 nm for cocrystal **1**; 346 nm for cocrystal **2**, 355 nm for cocrystal **3**, respectively. Both excitation and emission band passes were set at the adaptive width (20/5 nm for cocrystal **1**; 20/10 for cocrystal **2** and **3**). The delay time, gate time, and total decay time were set as 0.1, 0.5 and 50 ms, respectively. The phosphorescence decays were measured under the same conditions. Moreover, the total photo-luminescence (fluorescence and phosphorescence, abbreviated to fluo and phos, respectively) quantum yields (PLQY) in solid state were determined on an absolute PL quantum yield spectrometer (HAMAMATSU, Quantaurus-QY). PLQY of fluo and phos were calculated with total PLQY and relative PL area.

Fourier transform infrared analysis of the ground crystal powder was performed on an Avatar 360 FT-IR spectrophotometer (Nicolet Co.) with KBr pellets. The Raman spectra of the ground crystal powder were obtained with a Lab-RAM Aramis (HJY) Raman microscope using a He-Ne laser giving 633 nm radiation at the sample. The solid sample was detected directly with the resolution of better than 1 cm^{-1}, and scan rate of 20 scans per sample within 300 s.

Results and discussion

Phosphorescence spectra, decays and quantum yields.

In general, fluorescence could be easily observed for NHHs with π-conjugation system and rigid planar structure, while the phosphorescence emission is difficult to be obtained because of the spin-forbidden transitions between singlet and triplet states. Heavy atom effect is an efficient way to promote singlet-triplet conversion by enhancing spin-orbit coupling between the excited-state electrons of a compound and the massive nucleus of the heavy atom.[20-22] Herein it is expected that halogen bond as a strategy of introducing metal-free efficient heavy atom perturbers (*e.g.* 1,4-DITFB) in proper stoichiometry to the 3-R-NHHs crystals could induce the phosphorescence emission of cocrystals by efficient spin-orbital coupling.

Table 1 Crystal data and structure refinement.

Compound reference	1	2	3
CCDC no.	975980	975981	975982
Chemical formula	$C_{16}H_9F_2IN$	$C_{19}H_9F_4I_2N$	$C_{22}H_9F_6I_3N$
Formula Mass	380.14	581.07	782.00
Crystal system	Monoclinic	Monoclinic	Triclinic
Space group	P2(1)/c	P2(1)	P-1
a/Å	9.5953(7)	8.3207(7)	8.354(2)
b/Å	5.7426(4)	6.7511(6)	10.731(3)
c/Å	24.9356(17)	32.383(3)	12.901(3)
α/°	90	90.00	87.896(4)
β/°	95.9550(10)	96.561(2)	86.296(4)
γ/°	90	90.00	83.292(4)
V/Å3	1366.59(17)	1807.2(3)	1145.7(5)
T/K	295(2)	293(2)	295(2)
Z	4	4	2
No. reflections measured	7761	8914	5590
No. independent reflections	3151	5333	4098
R_{int}	0.0289	0.0280	0.0195
Final R_1 values	0.0313	0.0406	0.0351
Final $wR(F^2)$ values	0.0619	0.0791	0.0826
Final R_1 values	0.0443	0.0488	0.0443
Final $wR(F^2)$ values	0.0663	0.0826	0.0891
Absolute structure parameter	/	0.01(3)	/

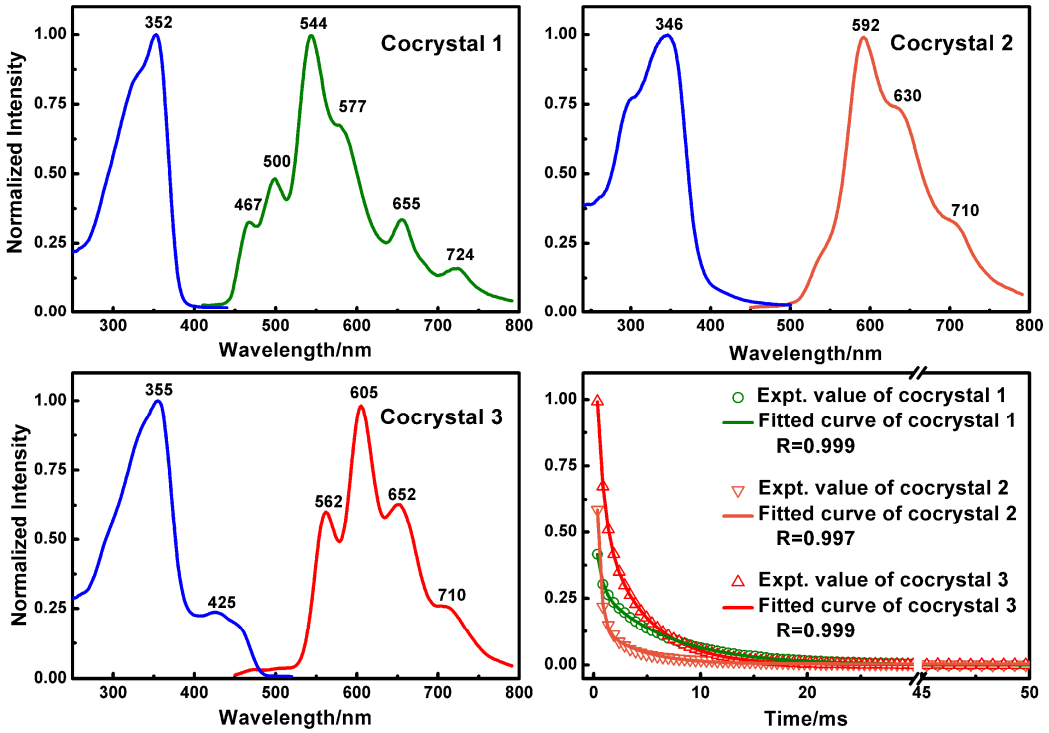

Fig. 1 The normalized phosphorescent excitation and emission spectra, and decay curves of cocrystals **1-3**. Excitation spectra: blue lines. Emission spectra: green, light red and red lines, respectively.

Fig. 2 Photographs of phosphorescent cocrystals **1-3** under 365 nm UV irradiation.

Table 2 The phosphorescent properties of cocrystals **1-3**.

	Phosphorescence spectra (λ/nm)		Decay (τ/ms)			PL Quantum yields (Φ)		
	λ_{ex}	λ_{em}	τ_1 (f_1/%)	τ_2 (f_2/%)	$\tau_{average}$	Fluo+Phos	Fluo	Phos
1	352	467, 500, 544 (max), 577, 655, 724	6.44 (52.6%)	0.48 (47.4%)	3.62	0.014	0.003	0.011
2	346	592 (max), 630 ,710	3.68 (11.4%)	0.34 (88.6%)	0.72	0.006	0.001	0.005
3	355	562, 605 (max), 652, 710	4.11 (42.8%)	0.62 (57.2%)	2.11	0.009	0.000	0.009

τ_1 and τ_2: the lifetime of long-lived and short-lived components; f_1 and f_2: the fractional contribution of long-lived and short-lived components; Fluo and Phos: fluorescence and phosphorescence.

Fig. 1 shows the normalized excitation and emission spectra of cocrystals **1-3**. It can be seen that the phosphorescence spectra go from 450 to near 800 nm with well-resolved vibrational fine-structures at 467, 500, 544 (max), 577, 655 and 724 nm for **1**, at 592 (max), 630 and 710 nm for **2**, at 562, 605 (max), 652 and 710 nm for **3**, when excited at 352, 346 and 355 nm, respectively. The luminescent photos of cocrystals **1-3** (**Fig. 2**) under UV 365 nm irradiation display the different colors corresponding to green, orange yellow and orange phosphorescence.

The phosphorescence decays of cocrystals were also investigated, as shown in **Fig. 1** and **Table 2**. The decay curves of all cocrystals obey the bi-exponential model. The phosphorescence lifetimes of cocrystals **1-3** are in ms scale with the average lifetimes of 3.62 ms, 0.72 ms and 2.11 ms, respectively. In addition, the absolute luminescence quantum yields of cocrystals **1-3** in the solid state were measured and listed in **Table 2**. Comparatively, cocrystals **1-3** are emissive with total quantum yields of 0.014, 0.006 and 0.009, and the main contribution to luminescence is from phosphorescence with the absolute quantum yields of 0.011, 0.005 and 0.009, respectively. Moreover, the average lifetime is relevant with the absolute quantum yield, namely, the average lifetime becomes longer with the increase of solid-state emission quantum yields.

Crystal structures and bonding models

XRD analysis reveals a 1:2 stoichiometry of donor to acceptor for cocrystal **1**, 1:1 for cocrystal **2** and 3:2 for cocrystal **3**, and their crystal structures are shown in **Fig. 3-5**. The 1D infinite chains of these cocrystals are all constructed mainly by C-I···N halogen bond. Other multiple interesting interactions, including C-H···I, C-H/I···π, C-H···F bonds and π-hole-π or π-π interaction[23], are also observed in these cocrystals, and the main bonding parameters are summarized in **Table S1**. All the bonding lengths are shorter than the sum of vdW radii of corresponding atoms, and the detailed information of their crystal structures are described as follows.

Cocrystal 1

XRD analysis reveals that the asymmetric unit has one half 1,4-DITFB molecule lying about an inversion centre and one PHN molecule in a general position in monoclinic cocrystal **1**. The 2D network structure is constructed by two cross-linked infinite supramolecular chains. Each chain is held together by C-I···N halogen bonds and C-H···F hydrogen bonds (*cf.* **Fig. 3**-c). Moreover, each molecule of 1,4-DITFB is surrounded by four PHN molecules to form a pair of A···B···A···B··· infinite chains along the axis. In turn, each PHN molecule is involved in the bonds with two neighbouring 1,4-DITFBs. In the cocrystal, the I1

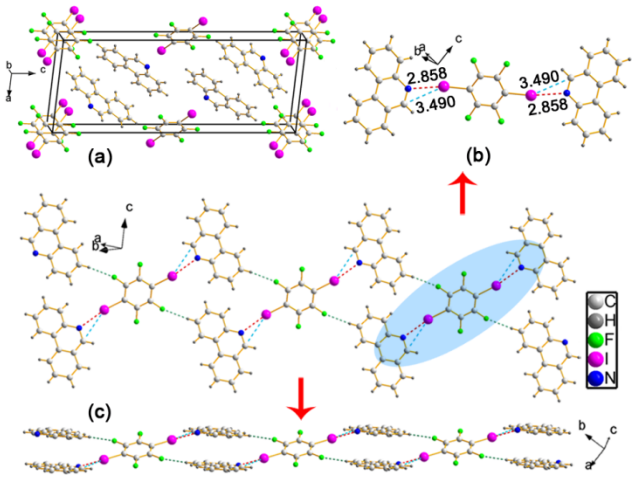

Fig. 3. The structure of cocrystal **1**. (a) Crystal cell unit. (b) The C-I···N halogen bonds in cocrystal **1**. (c) The 2D network structure of cocrystal **1** formed by C-I···N halogen bonds and C-H···F hydrogen bonds.

atom from 1,4-DITFB molecule interacts with the N1 atom to form C1-I1···N1 halogen bond. The C1-I1···N1 separation [for the N1 atom at (x, 1+y, z)] is 2.858(3) Å and the C1-I1···N1* angle is 169.68(11)°. The short distance of C1-I1···C16 contact should be a result impelled by the strong C1-I1···N1 halogen bond. When the 2D network structure is rotated by a certain angle, it can be seen clearly that 1,4-DITFB and PHN molecules locate in a corrugated plane, as shown in **Fig. 3c**-buttom. So, it can also be considered that the 2D network structure is constructed by two corrugated infinite chains.

Cocrystal 2

The whole construction of monoclinic cocrystal **2** is assembled by a series of infinite zigzag chains (*cf.* **Fig. 4c**). Each zigzag chain is connected by C-I···N, C-I···π, C-I···I and C-H···F bonds, and is further extended by the C-H···F hydrogen bonds to construct the complex 2D network. The asymmetric unit has two independent 1,4-DITFB molecules and two independent BfQ molecules with no imposed symmetry. For the basic bonding characters of the cocrystal structure, one I1/I4 atoms from 1,4-DITFB is bound to N2/N1 atom from BfQ molecule to form C1-I1···N2 and C10-I4···N1 halogen bonds, respectively. The C1-I1···N2 and C10-I4···N1 separations [for the N2 atom at (-x, 0.5+y, 1-z) and N1 atom at (1-x, -0.5+y, 2-z)] are 2.975(8) Å and 2.971(8) Å, the C1-I1···N2* and C10-I4···N1* angles are 171.6(3)° and 171.7(3)°, respectively. Simultaneously, the I3 atom considered as XB-acceptor and -donor is bound to the I2 atom from another 1,4-DITFB and C31 atom from BfQ to form C4-I2···I3 and C7-I3···π(C31) halogen bonds. The C4-I2···I3 and C7-I3···C31 separations [for the I3 atom at (x, y, z) and C31 atom at (1+x, y, z)] are 3.7858(9) Å and 3.628(11) Å, and the

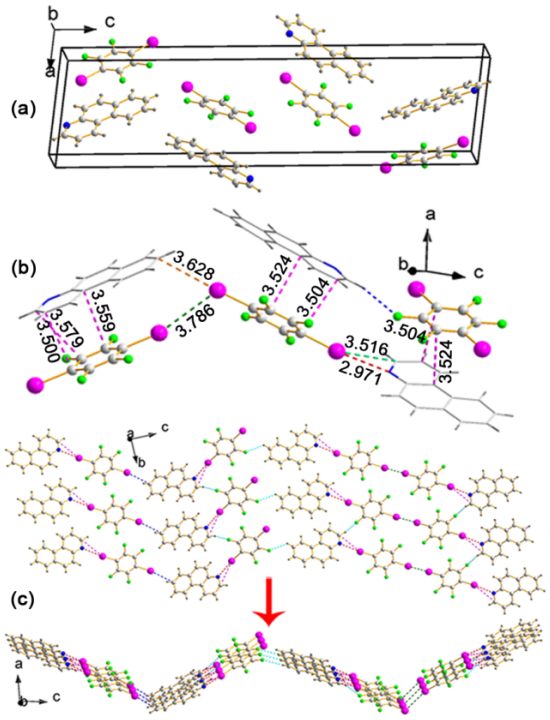

Fig. 4. The structure of cocrystal **2**. (a) Crystal cell unit. (b) The constitutional unit of 3D structure formed by C-I···N, C-I···π, C-I···I halogen bonds, C-H···F hydrogen bond and π-hole-π or π-π interactions in cocrystal **2**. (c) The 2D network structure of cocrystal **2**.

C4-I2···I3* and C7-I3···C31* angles are 166.3(2)° and 171.4(4)°, respectively, as shown in **Fig. 4b**. Such cooperative character of the iodine atom can be reasonable to describe the above system as $I_{XD}\cdots_{XA}I_{XD}\cdots\pi_{XA}$ pattern, where XD and XA represent XB-donor and -acceptor. Moreover, in 3D structure, BfQ and adjacent 1,4-DITFB form π-hole-π or π-π interactions. The shortest C-C (C1-C37) separation [for the C37 atom at (1+x, y, z)] is 3.500(13) Å and the corresponding dihedral angle is 4.1° (*cf.* **Fig. 4b**). Additionally, adjacent 1,4-DITFB and BfQ also form the C-H···F hydrogen bonds to keep auxiliary stability for the long chain.

Cocrystal 3

The cocrystal **3** with the simple tilted lattice pattern framework crystallizes in the monoclinic space group of P-1, where each lattice is constructed by four 1,4-DITFBs and four BhQ molecules (*cf.* **Fig. 5d**). Its asymmetric unit has one half 1,4-DITFB molecule lying about an inversion centre and one other 1,4-DITFB molecule and one BhQ molecule in general positions. The 1D infinite chain is constructed by C-I···π bonds in an over-the-bond pattern of I atom to the π-system (I atom is located above the C=C bond of BhQ molecule, expressed in **Fig. 5b**). The C1-I1···C14/C15 and C4-I2···C19/C20 separations [for the C14, C19 atoms at (x, y, 1+z) and C19, C20 atoms at (1+x, y, z)] are 3.564(6) and 3.492(6), or 3.536(6) and 3.651(6) Å, and the corresponding C-I···C* angles are 162.62(18)° and 174.50(19)°, or 167.37(19)° and 168.94(19)°, respectively. Then the 1D infinite chain is further extended by C7-I3···N1 and C20-H20···I2 bonds to give rise to a 2D network structure with numerous tilted lattices. Additionally, in each lattice, the F5 atom of 1,4-DITFB makes a short contact with the C12 atom at the *para*-position of N1 atom in BfQ molecule, the resulting F5-C12 separation is 2.955(6) Å. As a whole, each BhQ molecule can interact with adjacent 1,4-DITFB molecule to form C-I···π, C-I···N, C-H···I bonds and F-C contact, which can not only be helpful for stabilizing the complex structure, but also limit the rotation of BhQ molecule. On this basis, the 2D network is extended to 3D supramolecular structure using the above interactions.

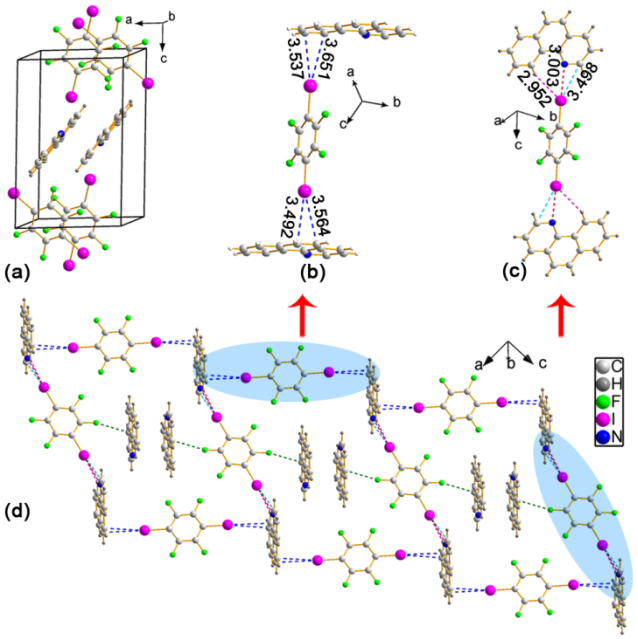

Fig. 5. The structure of cocrystal **3**. (a) Crystal cell unit. (b) and (c) The C-I···π and C-I···N, C-H···I bonds in cocrystal **3**. (d) The 3D network structure of cocrystal **3**.

In fact, it can be noticed from the above description on crystal structures that the N-position of three 3-RNHHs can regulate the interaction patterns of halogen bond and other interactions in cocrystal **1**, **2** and **3**. In cocrystal **1**, the N atom locates in convex position of the bent PHN molecule, which is the most suitable to form the strongest C-I···N halogen bond because of the minimum steric hindrance. When the N atom locates in flank position of the bent BfQ molecule in cocrystal **2**, the steric hindrance becomes little greater. And further, when the N atom locates in medial surface of the bent BhQ molecule in cocrystal **3**, the steric hindrance becomes the greatest. Therefore, the strength of C-I···N halogen bond becomes gradually weak from PHN to BhQ, the distance $d_{I\cdots N}$ changes are from 19.0%, 15.8% to 14.9% shorter than the sum of vdW radii of I and N atoms, respectively.

Moreover, as described above, three 3-R-NHHs in cocrystals are largely different with each other in phosphorescence property, and they also display larger red-shifts in phosphorescence spectra with respect to the same compounds on solid support under perturbation of heavy metal ions (510/495 nm for PHN, 510 nm for BfQ and 465/498/509 nm for BhQ, respectively).[21] For exploring the origination of the larger red-shifted phenomenon, it is necessary to study the characteristics of phosphorescence spectra of isolated PHN, BfQ and BhQ monomers. Herein one strategy was adopted to obtain the phosphorescence emitted from isolated free monomers using the hydrophobic cavity of *β*-cyclodextrin (*β*-CD) as compartmentation media and external heavy atom species to form an inclusion complex in which the phosphorescence can be induced by pure-physically extrinsic heavy atom effect.[24-26] As shown in **Fig. 6**, the phosphorescent peak positions of PHN (495 nm), BfQ (492 nm) and BhQ (491 nm) in *β*-CD aqueous solution induced by bromocyclohexane (Br-CH, as extrinsic heavy atom perturber) display no remarkable

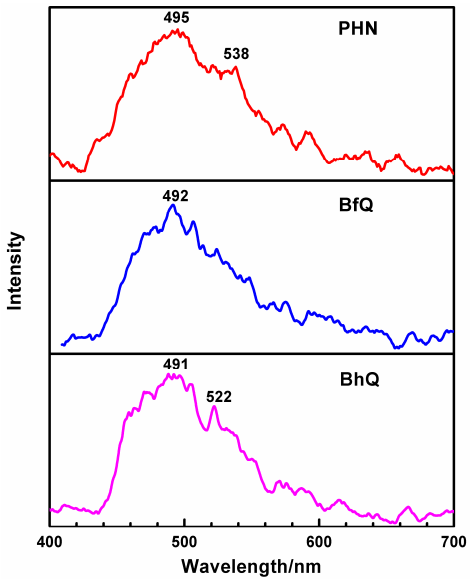

Fig. 6 The phosphorescence emission spectra of PHN, BfQ and BhQ induced by bromocyclohexane (Br-CH) in *β*-CD aqueous solution. Conditions: [PHN], [BfQ] and [BhQ], 5×10^{-5} mol·L^{-1}; [*β*-CD], 8×10^{-3} mol·L^{-1}; [Br-CH], 2×10^{-5} mol·L^{-1}. Excitation wavelengths are 285 nm, 280 nm and 265 nm, respectively, with the ex/em slits 20/20 nm.

difference at room temperature. Based on the above results, it can be concluded that the energy levels of the triplet state are lowered in the cocrystals as evidenced by the presence of a bathochromic effect in maximum emission bands of 50 ~ 100 nm.

The strong C-I···N halogen bond in the cocrystals must result in the lowest lying excited triplet states with ππ* property, from which the cocrystals produce phosphorescence. The different phosphorescence behaviours of three cocrystals lies in whether there is C-I···π halogen bond which makes the energy level of the lowest lying excited triplet states lower and the wavelength of phosphorescence emission spectrum longer. The other interactions as well as crystal environment in the cocrystals should contribute to the decrease of energy level of triplet state to a certain degree, too.

FT-IR and Raman

Interactions between 1,4-DITFB and bent 3-R-NHHs in the cocrystals were also investigated by FT-IR and Raman spectroscopy. The main bands of Raman and FT-IR spectra can be assigned to the respective vibrational modes of 1,4-DITFB and bent 3-R-NHHs, as shown in the **Fig. S1**. Although changes of the FT-IR and Raman spectra of cocrystals in many regions are not remarkable compared with the individual components, there are several significant differences that emphasize the presence of distinct interactions between the XB-donors and 3-R-NHHs.

For the XB-donors, in Raman, the active band at 158 cm^{-1} for free 1,4-DITFB is assigned to the combination of the symmetric C-I stretch and ring elongation, which slightly undergo a shift to lower frequency-shifts by 2 to 6 cm^{-1}. In FT-IR spectra, the fundamental band of ring sextant $\nu_{C\text{-}C}$ stretch generally occurs in 1600 ~ 1450 cm^{-1}, here it occurs at 1475 cm^{-1} (free) and 1460 or 1463 (bound), respectively, red-shifted by 12 ~ 15 cm^{-1}. This phenomenon can be ascribed to the electrostatic interaction. Because of the halogen bonds, the charge are more likely to transfer to the benzene ring, leading to the increase of electron density and the decrease of ring sextant $\nu_{C\text{-}C}$ stretch vibration frequency. Additionally, the active mode of C-F stretching of 1,4-DITFB at 947 nm also slightly downshifted by 2 to 5 cm^{-1}. All these data emphasize the presence of distinct halogen bonds between 1,4-DITFB and bent 3-R-NHHs.

Conclusions

Halogen bond as a good strategy to assemble controllable functional cocrystals was further proved here. XRD reveals that cocrystals **1-3** are successfully assembled by 1,4-DITFB and 3-R-NHHs (bent PHN, BfQ and BhQ) based on C-I···N, C-I···π or C-I···I bonds and other assisting weak interactions. The selected 3-R-NHHs are not phosphorescent in solid state, while they are differently emitting green, orange yellow and orange phosphorescence, respectively, in cocrystals **1-3**. And their phosphorescence are remarkably induced due to C-I···π halogen bond by which the spin-orbital coupling is more efficient. The different phosphorescence behaviours of cocrystals by interactions and diverse local molecular environment can provide some useful information for the design of strong phosphorescent cocrystals *via* halogen bonds from appropriate NHHs or polycyclic aromatic hydrocarbons (PAHs), and further enrich the practical application of the colorful phosphorescent cocrystals as

organic light-emitting diodes and photorefractive electroluminescent devices, *etc*, in the further research.

Acknowledgments

The authors thank the Natural Science Foundation of China (No.90922023) and Research Fund for the Doctoral Program of Higher Education of China (No.20110003110011) for the supports, and also appreciate very much the valuable suggestions and advices from reviewers and editor on this paper.

References

1 D. P. Yan, A. Delori, G. O. Lloyd, T. Friščić, G. M. Day, W. Jones, J. Lu, M. Wei, D. G. Evans and X. Duan, *Angew. Chem., Int. Ed.*, 2011, **50**, 12483.
2 Q. Feng, M. L. Wang, B. L. Dong, J. He and C. X. Xu, *Cryst. Growth Des.*, 2013, **13**, 4418.
3 D. P. Yan and D. G. Evans, *Mater. Horiz.*, 2014, **1**, 46.
4 J. A. Mikroyannidis, L. Fenenko and C. Adachi, *J. Phys. Chem. B*, 2006, **110**, 20317.
5 T. M. Figueira-Duarte and K. Müllen, *Chem. Rev.*, 2011, **111**, 7260.
6 K. C. Wu, P. J. Ku, C. S. Lin, H. T. Shih, F. I. Wu, M. J. Huang, J. J. Lin, I. C. Chen and C. H. Cheng, *Adv. Funct. Mater.*, 2008, **18**, 67.
7 C. J. Bhongale and C. S. Hsu, *Angew. Chem., Int. Ed.*, 2006, **45**, 1404.
8 G. R. Desiraju, P. S. Ho, L. Kloo, A. C. Legon, R. Marquardt, P. Metrangolo, P. Politzer, G. Resnati and K. Rissanen, *Prue Appl. Chem.*, 2013, **85**, 1711.
9 M. G. Chudzinski, C. A. McClary and M. S. Taylor, *J. Am. Chem. Soc.*, 2011, **133**, 10559.
10 F. Zapata, A. Caballero, N. G. White, T. D. W. Claridge, P. J. Costa, V. Félix and P. D. Beer, *J. Am. Chem. Soc.*, 2012, **134**, 11533.
11 V. Mugnaini, C. Punta, R. Liantonio, P. Metrangolo, F. Recupero, G. Resnati, G. F. Pedulli and M.Lucarini, *Tetrahedron Lett.*, 2006, **47**, 3265.
12 X. Pang, X. R. Zhao, H. Wang, H. L. Sun and W. J. Jin, *Cryst. Growth Des.*, 2013, **13**, 3739.
13 A. Priimagi, G. Cavallo, A. Forni, M. Gorynsztejn-Leben, M. Kaivola, P. Metrangolo, R. Milani, A. Shishido, T. Pilati, G. Resnati and G. Terraneo, *Adv. Funct. Mater*., 2012, **22**, 2572.
14 O. Bolton, K. Lee, H. J. Kim, K. Y. Lin and J. Kim, *Nat. Chem.*, 2011, **3**, 205.
15 D. Lee, O. Bolton, B. C. Kim, J. H. Youk, S. Takayama and J. Kim, *J. Am. Chem. Soc.*, 2013, **135**, 6325.
16 H. Y. Gao, Q. J. Shen, X. R. Zhao, X. Q. Yan, X. Pang and W. J. Jin, *J. Mater.Chem.*, 2012, **22**, 5336.
17 H. Y. Gao, X. R. Zhao, H. Wang, X. Pang and W. J. Jin, *Chin. J. Chem.*, 2013, **31**, 1279.
18 G. M. Sheldrick, *SHELXTL Version 5.1*, Bruker Analytical X-ray Instruments Inc., Madison, Wisconsin, USA, 1998.
19 G. M. Sheldrick, *SHELX-97, PC Version*, University of Gottingen, Germany, 1997.
20 J. C. Koziar and D. O. Cowan, *Acc. Chem. Res.*, 1978, **11**, 334.
21 T. Vo-Dinh, *Room Temperature Phosphorimetry for Chemical Analysis,* John Wiley & Sons, New York, 1984, ch. 1, pp. 13.
22 C. N. Burress, M. I. Bodine, O. Elbjeirami, J. H. Reibenspies, M. A. Omary and F. P. Gabbaï, *Inorg. Chem.*, 2007, **46**, 1388.
23 Herein a relatively "π-electron-deficient" system can be named π-hole because of its similarity with the σ-hole or π-hole proposed by Politzer et al. in ref. T. Clark, M. Hennemann, J. S. Murray and P. Politzer, *J. Mol. Model.*, 2007, **13**, 291; P. Politzer, J. S. Murray and T. Clark, *Phys. Chem. Chem. Phys.*, 2013, **15**, 11178.
24 S. Scypinski and L. J. Cline Love, *Anal. Chem.*, 1984, **56**, 322.
25 S. Hamai, *J. Am. Chem. Soc.*, 1989, **111**, 3954.
26 A. M. de la Peña, I. Durán-Merás, F. Salinas, *Anal. Chim. Acta*, 1991, **255**, 351.